Excited State Characteristics of 6-Azauracil in Acetonitrile: Drastically Different Relaxation Mechanism from Uracil

Takashi Kobayashi, Yosuke Harada, Tadashi Suzuki,* and Teijiro Ichimura

Department of Chemistry and Materials Science, Tokyo Institute of Technology, 2-12-1 Ohokayama, Meguro-ku, Tokyo 152-8551, Japan

Received: April 10, 2008; Revised Manuscript Received: September 22, 2008

Excited-state dynamics of 6-azauracil (6-AU) and sensitized singlet oxygen formation in acetonitrile solution with UV irradiation were investigated for the first time. In the transient absorption measurement, the 248 nm laser photolysis gave a relatively intense absorption band at 320 nm ($\epsilon = 1100 \pm 100$ dm^3 mol^{-1} cm^{-1}) and a broadband in the 500 − 700 nm region due to triplet 6-AU. The triplet 6-AU, decaying with the rate constant of $(5.3 \pm 0.2) \times 10^6$ s^{-1} in Ar saturated acetonitrile, was quenched by molecular oxygen with the rate constant of $(2.5 \pm 0.1) \times 10^9$ dm^3 mol^{-1} s^{-1}. The formation quantum yield of excited triplet 6-AU was estimated to be unity by acetone triplet sensitization and actinometry with benzophenone. The time-resolved thermal lensing signal of 6-AU was also observed by 248 nm laser excitation. In the presence of molecular oxygen, the sensitization from triplet 6-AU gave rise to formation of singlet oxygen O_2 ($^1\Delta_g$) with a quantum yield of 0.63 ± 0.03. Drastically different excited-state dynamics of aza-substituted uracil from normal uracil were clarified, and the mechanism for the enhancement of intersystem crossing by aza-substitution is discussed.

Introduction

Nucleic acids, DNA and RNA, are fundamental materials for all living organisms because of protein synthesis and genetic information storage. Nucleic acid bases (adenine, guanine, cytosine, thymine and uracil) serve as chromophores absorbing radiation below 300 nm.[1] Several phenomena result from light absorption by nucleic acid bases such as the DNA photodamage and the photoreactivation. Studies on excited states of nucleic acid bases are essential and important to understand such phenomena. In general, nucleic acid bases are exceedingly stable to photochemical pathways that inflict lethal damage to DNA, because the bases in the excited singlet states exhibit a remarkably rapid decay into the ground (S_0) state.[2] To clarify the excited-state dynamics of the nucleic acid bases, many researches with ultrafast spectroscopy and quantum chemical calculations have been carried out in recent years.[2−14] The existence of near barrier-less paths that imply important ring deformation connecting the excited-state to the S_0 state through a conical intersection state was proposed.[3,4,6−10,13,14] However, the mechanism responsible for the ultrafast nonradiative deactivation has not been understood completely yet.

Analogues of nucleic acid bases having a similar molecular structure show distinct biochemical properties relative to the parent nucleic acid bases. The biochemical effects of these analogues have been studied and some were found to be useful for antivital,[15] anticancer[16] therapies, and so on. On the other hand, the excited-state of analogues of nucleic acid bases has been attracting attention in recent years. In our recent work, the excited-state dynamics of 4-thiothymidine, a thio-substituted thymidine, was studied.[17] The excited-state dynamics of 4-thiothymidine are drastically different from thymidine with high yields for intersystem crossing (ISC) (1.0 ± 0.1) and the singlet oxygen O_2 ($^1\Delta_g$) formation (0.50 ± 0.10). For normal thymidine, the main excited-state decay process is internal conversion into the S_0 state.[1] In fact, the relaxation dynamics of nucleic acid base are sensitive to substitution, therefore, investigating the effect of the substitution is very interesting and fruitful.

CHART 1: Schematic Structure of 6-AU, Uracil, and Thymine

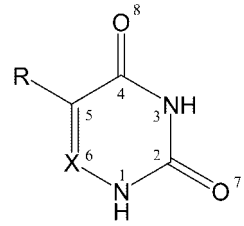

	R	X
6-AU	H	N
Uracil	H	C-H
Thymine	CH_3	C-H

Aza-nucleic acid bases, with a nitrogen atom inserted into the nucleic acid base skeleton, are analogues well-known for their antineoplastic and fungistatic properties.[18,19] Particularly, biological effects of 6-azauracil (6-AU, Chart 1) have been extensively investigated. It was shown to inhibit animal tumors,[20] human acute leukemia,[21] and the growth of a large number of microorganisms.[22] Despite the accumulated knowledge about biological effects and medical applications, the excited-state dynamics of 6-AU have not been clarified yet. The 6-AU molecule has an N atom inserted into the C═C double bond of uracil. Quantum chemical calculation suggested that the C═C double bond would play an important role of the ultrafast relaxation of uracil.[3,4,6−9] Thus, it is interesting to clarify the electronic configuration and the excited-state dynamics of 6-AU. The information on the excited-state characteristics of 6-AU will let us understand the unique relaxation dynamics of the normal nucleic acid bases.

It is also known that the solvent molecule would affect the relaxation dynamics of the excited nucleic acid bases. Gas phase studies have shown that the addition of water molecule should greatly accelerate the internal conversion to the ground-state of uracil derivatives.[12] The photoaddition reaction in the aqueous solution of 6-AU was reported.[23] In acetonitrile, polar but aprotic solvent, we could exclude the formation of solute/solvent

* Corresponding author.

10.1021/jp803096j CCC: $40.75
Published on Web 12/03/2008

hydrogen bonds and the influence of the photoreaction and investigate the intrinsic excited-state dynamics of the nucleic acid bases. In this article, the excited-state dynamics of 6-AU in acetonitrile was investigated by means of laser flash photolysis and time-resolved thermal lensing (TRTL) techniques. The TRTL method is a powerful photothermal technique used to explore nonradiative deactivation processes of photoexcited molecules.[24−28] The relaxation mechanism of 6-AU is discussed in detail in comparison with uracil.

Experimental Section

Materials. 6-AU, uracil, and acetone were purchased from Sigma Aldrich and used without further purification. 2-Hydroxybenzophenone and benzophenone (Tokyo Kasei, GR grade) were purified by recrystalization several times with methanol and hexane. Acetonitrile (Kanto Chemical, GR grade) was used from a freshly opened bottle. Sample solutions were deaerated by bubbling with Ar gas or flushed with O_2 gas for 30 min.

Apparatus. For the transient absorption measurement, a KrF excimer laser (Lambda Physik, COMPex102; 248 nm, 350 mJ/pulse, 30 ns pulse duration) or a XeCl excimer laser (Lambda Physik, COMPex102; 308 nm, 200 mJ/pulse, 20 ns pulse duration) was used as an excitation light source and a Xe flash lamp (Ushio, UXL-300DO; 300 W) was used as a monitoring light source.

The detailed experimental procedure for the TRTL measurement has been described elsewhere.[26] Briefly, the KrF excimer laser was used as an excitation light source. The excitation laser power, attenuated through a variable reflective neutral density filter (Sigma Koki, VND-100), was monitored by a silicon photodiode (Hamamatsu Photonics, S1336−5BQ) calibrated with a pyroelectric detector (Gentec, ED100). A cw beam of a He−Ne laser (Uniphase, 1103P; 2 mW), used for probing of the lens signal, was focused in front of a sample cell (NSG, T-59FL-10; 10 mm optical pass length) with a 100 mm focal length lens collinearly to the excitation laser pulse. The probe beam sampled through a pinhole (Corion, 2401; 300 μm diameter) and a monochromator (Nikon, P-250) was detected by a photomultiplier tube (Hamamatsu Photonics, R928). The output signal converted into the voltage with a 500 Ω load resister was fed to a digital oscilloscope (Sony Tektronix, TDS380P; 400 MHz, 2 GS/s) and transferred to a personal computer. The signal was averaged over 50 shots to improve the S/N ratio.

The sample solution was flowed into the cuvette to remove the influence of photoproducts. With 30 min O_2 bubbling, the sample solution was considered to be O_2 saturated. Since additional bubbling made no change of triplet lifetime. The O_2 concentration of the air- and O_2 saturated sample solution was according as the literature value.[29] All the measurements were carried out at room temperature.

The emission of $^1O_2$* ($^1\Delta_g$) was detected through a glass filter (Toshiba, IR-D80A) with an InGaAs PIN photodiode (Hamamatsu Photonics, G8376−05) and a handmade amplifier.

The UV absorption spectrum was measured with a double beam spectrometer (Jasco, Ubest V-550). The emission and the fluorescence excitation spectra were measured by a spectrofluorometer (Jasco FP-6500).

Theoretical Calculation. Becke's three-parameter hybrid functional and Lee−Yang−Parr correlation functions (B3LYP) were adopted. A 6-31G(d,p) basis set was used for the geometry optimization calculations. Vertical transition energies and oscillator strengths of the excited singlet and the triplet states of 6-AU were calculated by time-dependent density functional theory (TD-DFT), using the optimized geometry of the S_0 state. Solvent effects were computed using the polarized continuum model (PCM).[30,31] The GAUSSIAN 03 suite of programs[32] was used for the calculations.

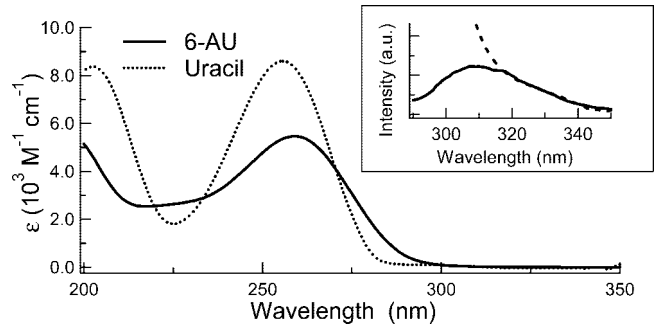

Figure 1. Absorption spectra of 6-AU (solid line) and uracil (dotted line) in acetonitrile. Inset: Excitation spectrum (solid line) and absorption spectra (broken line) of 6-AU in acetonitrile. Monitoring wavelength for the excitation spectrum was 420 nm (bandwidth = 5 nm).

TABLE 1: Ground State Absorption Spectrum, Calculated Vertical Excitation Energies (E_{calc}), and Oscillator Strengths (f_{calc}) of Excited Singlet and Triplet States of 6-AU in Acetonitrile

		λ_{max}[a]/ nm (cm^{-1})	ϵ[b]/dm^3 $mol^{-1}cm^{-1}$	E_{calc}[c,d]/ cm^{-1}	f_{calc}[c]
S_1	$^1n\pi^*$			33 100	0.0003
S_2	$^1\pi\pi^*$	259 (38610)	5470	37 880	0.1221
S_3	$^1n\pi^*$			37 990	0.0016
S_4	$^1\pi\pi^*$	229 (43670)	2660	43 510	0.0674
T_1	$^3\pi\pi^*$			24 180	
T_2	$^3n\pi^*$			28 710	
T_3	$^3\pi\pi^*$			34 040	
T_4	$^3n\pi^*$			34 830	

[a] The peak wavelengths of absorption. [b] The molar absorption coefficient at the absorption peak. [c] Calculated by TD-DFT method for the molecular structure in the S_0 state optimized at the B3LYP/6-31G(d,p) level. [d] The values scaled by 0.95.

Results and Discussion

Molecular Structure and Electronic Configuration of the Excited States of 6-AU. Figure 1 shows the absorption spectrum of 6-AU in acetonitrile. For comparison, the spectrum of uracil is also shown. Both compounds showed two characteristic absorption bands near 260 and 200 nm. The intense absorption band of uracil near 260 nm was shown to be a $\pi\pi^*$ transition,[8] so that the corresponding band of 6-AU was tentatively assigned to a $\pi\pi^*$ transition. Though we measured the emission spectrum of 6-AU, no emission was observed with 248 nm excitation at room temperature. The result suggests the quantum yield for fluorescence (Φ_F) from the excited singlet state to the S_0 state should be quite low. On the other hand, a weak emission was observed by the 308 nm light excitation. The emission peak was at 420 nm. The excitation spectrum was shown in Figure 1 inset. This weak emission by the 308 nm light excitation is discussed below. Values of wavelengths of absorption peaks and molar absorption coefficients for 6-AU in acetonitrile are summarized in Table 1.

The optimized geometry of 6-AU and uracil computed in acetonitrile are shown in Figure 2. The bond lengths and the angles for the two compounds are also shown. Our calculation indicates that the 6-AU molecule should have a C5═N6 double

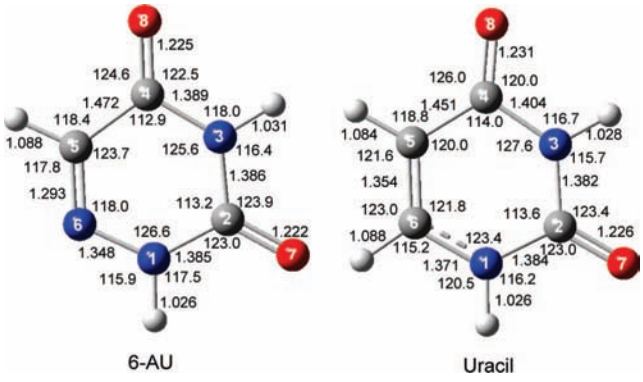

Figure 2. Optimized geometries, the bond lengths (Å), and the angles (degree) of 6-AU (left) and uracil (right) computed in acetonitrile.

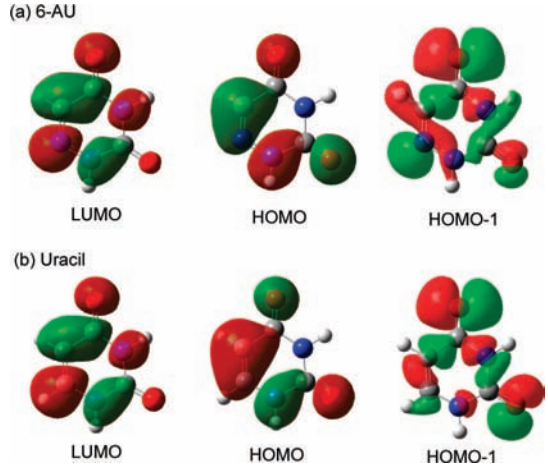

Figure 3. Description of HOMO, LUMO and HOMO-1 for (a) 6-AU and (b) uracil involved in the HOMO−LUMO ($\pi\pi^*$) and HOMO-1/LUMO ($n\pi^*$) electronic transitions.

bond of 1.293 Å shorter than a C5═C6 double bond of uracil (1.354 Å). These calculated bond lengths agree well with the result of the X-ray structure analysis (1.291 Å and 1.340 Å, respectively).[33]

Figure 3 shows the molecular orbitals (MOs) of 6-AU and uracil. The features of LUMO, HOMO, and HOMO-1 of uracil well agreed with the ones reported previously.[9] The HOMO and the LUMO of 6-AU have almost the same shape with those of uracil, respectively. However, the HOMO-1 of 6-AU has a different feature from that of uracil. The lone pair orbital of N6 contributes to the HOMO-1 for 6-AU.

In the Franck−Condon region of both 6-AU and uracil, the first excited singlet (S_1) state arises mainly from the HOMO-1 → LUMO transition, which has a $n\pi^*$ character, whereas the second excited singlet (S_2) state predominantly has the HOMO → LUMO transition, which has a $\pi\pi^*$ character. The vertical transition energies from the S_0 state to the S_1 and the S_2 states of 6-AU are calculated to be 33000 cm^{-1} and 38000 cm^{-1} (scaled by 0.95) respectively (S_1 = 38000 cm^{-1}; S_2 = 40000 cm^{-1} for uracil, also scaled by 0.95). The calculation also indicated that the lowest excited triplet (T_1) state of 6-AU and uracil should possess a $\pi\pi^*$ character that lies about 8900 cm^{-1} and 11000 cm^{-1} below the S_1 state, respectively. The energy difference between the S_1 and the T_1 states of 6-AU is smaller than that of uracil by about 2000 cm^{-1} in the Franck−Condon region. The transition energies and the oscillator strength of the excited states of 6-AU obtained by the TD-DFT calculations are summarized in Table 1.

Transient Absorption Spectrum and Decay Time Profile of Triplet 6-AU. To obtain the spectral and kinetic information including the triplet state of 6-AU, laser flash photolysis was utilized to measure transient absorption of 6-AU. Figure 4a shows the transient absorption spectrum of 6-AU in Ar-saturated acetonitrile ([6-AU] = 2.2×10^{-4} mol dm^{-3}) obtained immediately after the 248 nm laser irradiation. A relatively intense absorption band at 320 nm and a broadband at 500−700 nm were observed. The transient absorption spectrum of uracil is also shown in the inset. In the region from 300 to 450 nm, the spectral features are similar with the triplet−triplet (T−T) absorption spectra of uracil reported.[34]

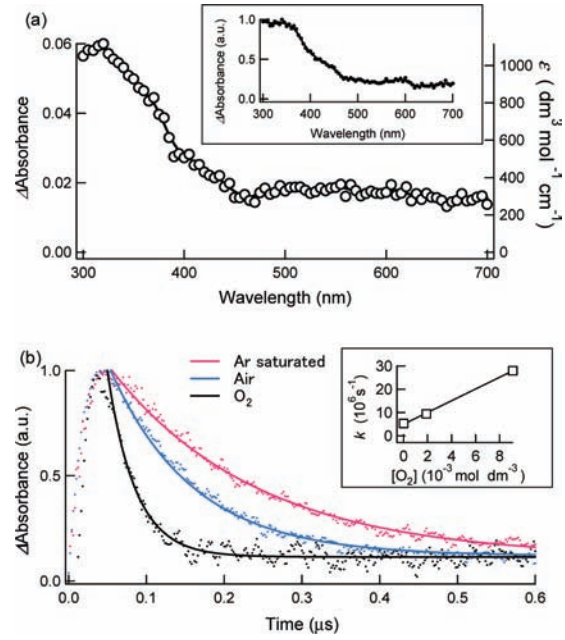

Figure 4. (a) Transient absorption spectrum of 6-AU in Ar-saturated acetonitrile obtained immediately after the 248 nm laser irradiation. Inset: Transient absorption spectrum of uracil in Ar-saturated acetonitrile obtained immediately after the 248 nm laser irradiation. (b) Time profiles of the transient absorption of 6-AU monitored at 320 nm in Ar-saturated (red), air-saturated (blue), O_2-saturated (black) acetonitrile. The solid lines denote the analytical results obtained with the single-exponential equations. Inset: Plots of the decay rate constant of the transient absorption at 320 nm against the concentration of dissolved oxygen ($[O_2]$). The solid line designates the fitting line by least-squares method. The O_2 concentration of the sample solution was estimated by the literature value.[29]

Figure 4b shows the time profiles of the transient absorption at 320 nm. The absorption decayed with the first-order kinetics, and the decay rate constant was estimated to be $(5.3 \pm 0.2) \times 10^6$ s^{-1}. The rate constant does not depend on the monitoring wavelength. Similar measurements were performed in air- or O_2-saturated acetonitrile solution. The spectrum obtained under the air- or the O_2-saturated condition corresponds to that in the Ar-saturated solution, but the lifetime of the transient decreased with increasing O_2 concentration $[O_2]$ (Figure 4b). The quenching rate constant (k_q) by O_2 was successfully determined to be $(2.5 \pm 0.1) \times 10^9$ dm^3 mol^{-1} s^{-1} (Figure 4b inset), taking into account of the concentration of the dissolved molecular oxygen in acetonitrile.[29]

As the transient was effectively quenched by O_2, and the spectral feature was similar with the T–T absorption spectrum of uracil (inset in Figure 4a), the spectrum was assigned to the absorption of triplet 6-AU (^{3}6-AU*). The decay rate constants of triplet 6-AU and uracil and the bimolecular quenching rate constants by O_2 are summarized in Table 2.

TABLE 2: Decay Rate Constants of 6-AU and Uracil in Acetonitrile and Their Bimolecular Quenching Rate Constants by Oxygen

	k_0[a]/10^5 s^{-1}	k_q[b]/10^9 dm^3 mol^{-1} s^{-1}	ref
6-AU	53 ± 2	2.5 ± 0.1	this work
Uracil	7.0 ± 0.2[c]	6.3 ± 0.1	this work
	5.0	3.9[d]	34, 35

[a] Rate constant of the triplet unimolecular decay. [b] Bimolecular quenching rate constant of the triplet by oxygen. The O_2 concentration of the sample solution was estimated by the literature value.[29] [c] The self-quenching of triplet uracil by the parent molecule in the ground-state was reported. This unimolecular decay rate constant of triplet uracil was estimated with the T–T absorption decay rate constant, the rate constant of the self-quenching (2.0×10^9 dm^3 mol^{-1} s^{-1}),[34] and the concentration of uracil (1.5×10^{-4} mol dm^{-3}). [d] The value was obtained in aqueous solution.[35]

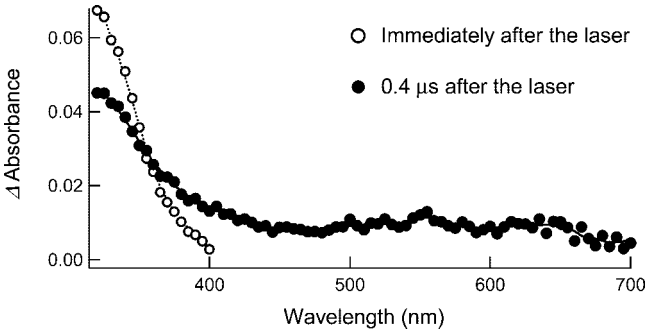

Figure 5. Transient absorption spectra of acetone (3.7×10^{-2} mol dm^{-3}) containing 6-AU (1.2×10^{-3} mol dm^{-3}) in acetonitrile obtained immediately (open circle) and at 0.4 μs (closed circle) after the 308 nm laser excitation.

Determination of the Quantum Yield (Φ_{ISC}) for Singlet → Triplet ISC by Acetone Sensitization and Actinometry with Benzophenone. To obtain the information on the triplet characterization, triplet sensitization experiments were carried out with acetone. Acetone is a suitable sensitizer because the triplet absorption spectrum is well-known and its triplet energy (337 kJ mol^{-1})[36] is sufficiently higher than that of 6-AU estimated by the phosphorescence spectrum measurement (234 kJ mol^{-1}).[37] Figure 5 shows transient absorption spectra of the 6-AU (1.2×10^{-3} mol dm^{-3})−acetone (3.7×10^{-2} mol dm^{-3}) system in Ar-saturated acetonitrile obtained by the 308 nm excitation. The acetone molecule could be assumed as the only absorber for the 308 nm light in this system since 6-AU has very low molar absorption coefficient at this wavelength and low concentration relative to acetone. An absorption band in the wavelength region of 320−400 nm appeared immediately after the laser irradiation, which is attributed to the T–T absorption of acetone.[36] At 0.4 μs after the laser, a new broad absorption band emerged in the 320−700 nm region. The spectral feature at 0.4 μs after the laser is identical to that with the 248 nm direct excitation (Figure 4a). These experimental facts apparently indicate that energy transfer from triplet acetone (^{3}Ace*) to 6-AU takes place to produce ^{3}6-AU*. Therefore, the transient species observed in Figure 4 is certainly assigned to ^{3}6-AU*.

Figure 6 shows the time profiles of the transient absorption monitored at 600 nm for various concentrations of 6-AU [6-AU] where ^{3}Ace* has no absorption band.[36] The rise and decay feature due to production and disappearance of ^{3}6-AU* was clearly observed. The reaction scheme of triplet sensitization between acetone and 6-AU is described as follows.

$$\mathrm{Ace} \xrightarrow{h\nu,\ \mathrm{ISC}} {}^3\mathrm{Ace}^*$$

$${}^3\mathrm{Ace}^* \xrightarrow{k_0} \mathrm{Ace}$$

$${}^3\mathrm{Ace}^* + \text{6-AU} \xrightarrow{k_q[\text{6-AU}]} {}^3\text{6-AU}^* + \mathrm{Ace}$$

$${}^3\text{6-AU}^* \xrightarrow{k_{6\text{-AU}}} \text{6-AU}$$

Here k_0 is the unimolecular decay rate constant of ^{3}Ace* in the absence of 6-AU, k_q is the bimolecular quenching rate constant of ^{3}Ace* by 6-AU, and $k_{6\text{-AU}}$ is the decay rate constant of ^{3}6-AU*. Assuming that the energy transfer efficiency from ^{3}Ace* to 6-AU is unity, the time-evolution of absorbance at 600 nm, ΔA_{600}^{6-AU}, can be described as follows:

$$\Delta A = C\{\exp(-k_{6-AU}t) - \exp(-k_t t)\} \quad (1)$$

$$k_t = k_0 + k_q[\text{6-AU}] \quad (2)$$

$$C = k_q[6-\mathrm{AU}]\varepsilon_{600}^{6-AU}\Delta A_{325}^{Ace}/(k_t - k_{6-AU})\varepsilon_{325}^{Ace} \quad (3)$$

where ΔA_{325}^{Ace} is the absorbance of ^{3}Ace* at 325 nm immediately after the laser irradiation, ε_{600}^{6-AU} is the molar absorption coefficient of ^{3}6-AU* at 600 nm, and ε_{325}^{Ace} is the molar absorption coefficient of ^{3}Ace* at 325 nm. Since the molar absorption coefficient of ^{3}Ace* at 325 nm in acetonitrile is not known, it was determined with benzophenone (BP) as an actinometer ($\Phi_{ISC}^{BP} = 1$, $\varepsilon_{520}^{BP} = 6500$ dm^3 mol^{-1} cm^{-1})[29,38] to be 610 ± 70 dm^3 mol^{-1} cm^{-1}.

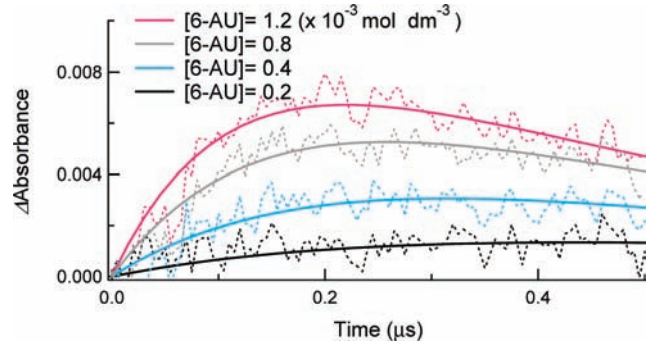

Figure 6. Time profiles of the transient absorption monitored at 600 nm of acetone (3.7×10^{-2} mol dm^{-3}) containing 6-AU (1.2×10^{-3} mol dm^{-3} (red), 0.8×10^{-3} mol dm^{-3} (gray), 0.4×10^{-3} mol dm^{-3} (blue), and 0.2×10^{-3} mol dm^{-3} (black)) in Ar-saturated acetonitrile obtained after the 308 nm excitation. The solid line designates the best fitting line obtained with eq 1.

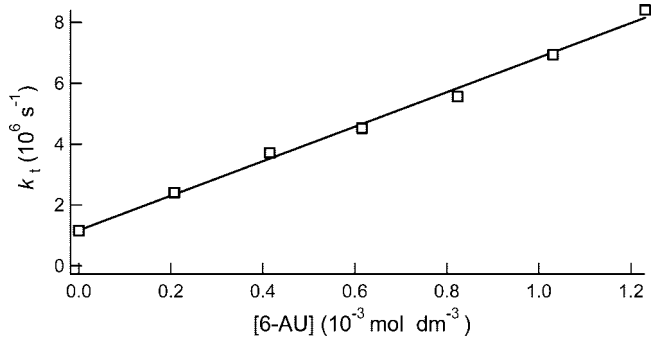

Figure 7. Stern−Volmer plots of the k_t value as a function of [6-AU] obtained by the 308 nm laser excitaion in acetonitrile. The k_t value corresponding to [6-AU] = 0 is the decay rate constant of the transient absorption of ^{3}Ace* without 6-AU monitored at 325 nm. The solid line designates the best fitting line obtained with eq 2.

TABLE 3: Photophysical Properties of 6-AU and Uracil in Acetonitrile

	λ_{max}[a]/nm	ϵ_{TT}[b]/dm^3 mol^{-1} cm^{-1}	Φ_{ISC}[c]	Φ_{Δ}[d]
6-AU	320	1100	1.00	0.63 (0.34)[e]
uracil	340	2750[f]	0.21	0.13[g]

[a] Peak wavelength of T−T absorption. [b] Molar absorption coefficient of the triplet at the maximum wavelength. [c] Quantum yield for singlet → triplet intersystem crossing. [d] Quantum yield for generation of $O_2(^1\Delta_g)$ via photosesitization under the O_2 saturated condition. [e] The value in parentheses was obtained under aerated condition. [f] Reference 34. [g] Reference 42. The value was obtained under aerated conditions.

Figure 7 shows Stern−Volmer plots of the formation rate constant of ^{3}6-AU* (k_t) against [6-AU]. The solid line indicates the best fitting curve. The quenching rate constant of ^{3}Ace* by 6-AU was determined to be $(5.7 \pm 0.3) \times 10^9$ dm^3 mol^{-1} s^{-1}. This value is close to the diffusion rate constant in acetonitrile (1.9×10^{10} dm^3 mol^{-1} s^{-1}).[29]

The molar absorption coefficient of ^{3}6-AU* was provided by analyzing the time profile of the transient absorption of ^{3}6-AU* (Figure 6) with eq 1-3. ε_{600}^{6-AU} was successfully determined to be 320 ± 30 dm^3 mol^{-1} cm^{-1} and ε_{320}^{6-AU} was 1100 ± 100 dm^3 mol^{-1} cm^{-1}. The molar absorption coefficient of ^{3}6-AU* was smaller than that of uracil ($\varepsilon_{340}^{Uracil} = 2750$ dm^3 mol^{-1} cm^{-1}).[34] The quantum yield of ISC for 6-AU in acetonitrile will be obtained with the molar absorption coefficient.

The quantum yield of ISC for 6-AU can be determined by comparative actinometry with BP,

$$\Phi_{ISC}^{6-AU} = \frac{\Delta A_{320}^{6-AU}/\{I_L^{6-AU}(1-10^{-A^{6-AU}})\}}{\Delta A_{520}^{BP}/\{I_L^{BP}(1-10^{-A^{BP}})\}}(\varepsilon_{520}^{BP}/\varepsilon_{320}^{6-AU})\Phi_{ISC}^{BP} \quad (4)$$

where ΔA_{320}^{6-AU} and ΔA_{520}^{BP} are absorbances of the T−T absorption of 6-AU and BP at $t = 0$, Φ_{ISC}^{6-AU} and Φ_{ISC}^{BP} are the quantum yields for ISC of 6-AU and BP, and ε_{320}^{6-AU} and ΔA_{500}^{BP} are the molar absorption coefficient of triplet 6-AU and BP, respectively. I_L is the incident laser power, A is the absorbance of the sample at the excitation wavelength (248 nm), and the $1-10^{-A}$ term represents the absorptivity of the sample at 248 nm. From the ratio between the two values of $\Delta A/\{ I_L(1-10^{-A})\}$ (0.17 ± 0.01), Φ_{ISC}^{6-AU} was successfully obtained to be 1.00 ± 0.10. The quantum yield for ISC of uracil was also estimated by comparison between the intensity of the T–T absorption of uracil and 6-AU under the same experimental condition (data not shown). Applying the literature value of the molar absorption coefficient of the excited triplet state uracil ($\Phi_{ISC}^{Uracil} = 2750$ dm^3 mol^{-1} cm^{-1}),[34] Φ_{ISC}^{Uracil} was obtained to be 0.21 ± 0.02. This value agrees well with the literature value ($\Phi_{ISC}^{Uracil} = 0.2$).[34] In fact, Φ_{ISC}^{6-AU} value is about five times larger than that of uracil in acetonitrile. Thus, aza-substitution results in a drastic change in uracil excited-state dynamics. Photophysical properties of 6-AU and uracil are summarized in Table 3.

An Estimation of the Quantum Yield of Singlet Oxygen Formation by Sensitization of Triplet 6-AU with TRTL Measurements. Since Φ_{ISC} of 6-AU is unity and ^{3}6-AU* is quenched by dissolved molecular oxygen, a sensitization reaction between ^{3}6-AU* and molecular oxygen should occur. We carried out the TRTL measurement to detect singlet oxygen, O_2 ($^1\Delta_g$). Because the emission quantum yield of O_2 ($^1\Delta_g$) is quite low (7.1×10^{-5}),[39] the TRTL method is a powerful tool to quantitatively obtain the formation yield.[17] Figure 8 shows

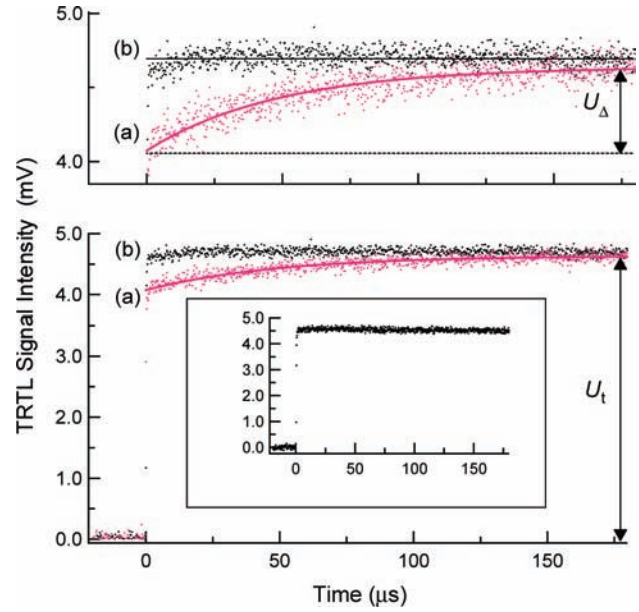

Figure 8. Time profiles of the TRTL signal of (a) 6-AU and (b) 2-HBP in O_2-saturated acetonitrile excited at 248 nm. Expanded view of the new heat component U_Δ is depicted in the upper panel. The solid line in part (a) shows the fitting line with a single-exponential equation. The flat line shows $\alpha = 1$, determined by the result of the TRTL measurement of 2-HBP. Inset: Time profile of the TRTL signal of 6-AU in Ar-saturated acetonitrile excited at 248 nm.

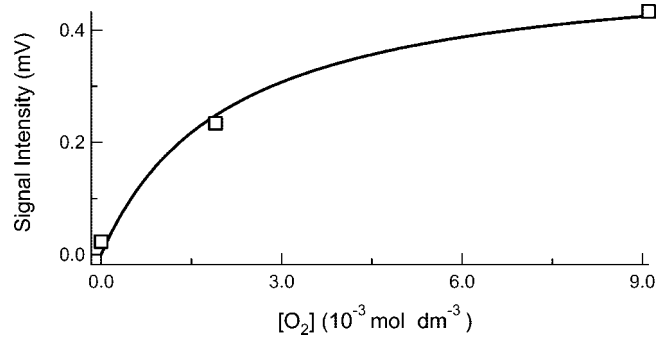

Figure 9. Plots of the signal intensity of emission in near-IR region (1100−1400 nm) of 6-AU in Ar-saturated, air-saturated, and O_2-saturated acetonitrile observed by the 248 nm laser excitation. The solid line designates the best fitting line obtained with eq 7.

the TRTL signals of 6-AU in acetonitrile with the 248 nm laser excitation under the Ar or the O_2 saturated condition in the 200 μs time window. The TRTL signal for 2-hydroxybenzophenone (2-HBP) is also presented in Figure 8. 2-HBP is a well-known calorimetric standard, which emits all the energy absorbed as heat into the solvent within a single laser pulse.[40] Under the Ar saturated condition the TRTL signal of 6-AU rose up steeply, so that all relaxation processes have been completed within our instrumental time resolution (300 ns) (inset in Figure 8). In contrast, under the O_2 saturated condition, a new rising heat component (U_Δ) was observed. The U_Δ component increased single-exponentially, and the rate constant was obtained to be $(1.7 \pm 0.1) \times 10^{-4}$ s^{-1}. This U_Δ component should result from the heat released through the O_2 ($^1\Delta_g$) deactivation. To confirm the formation of O_2 ($^1\Delta_g$), we tried to detect near-IR emission of O_2 ($^1\Delta_g$) with an InGaAs PIN photodiode. Figure 9 shows the IR emission intensity against the concentration of oxygen dissolved in acetonitrile ([O_2]) with the 248 nm irradiation. The signal intensity increased with increasing [O_2]. Thus, the formation of O_2 ($^1\Delta_g$) sensitized by ^{3}6-AU* has been surely confirmed.

Quantitatively, to obtain the yield of O_2 ($^1\Delta_g$) formation, we analyzed the TRTL signal precisely. The TRTL signal U is defined as

$$U = KI_L\alpha(1 - 10^{-A}) \quad (5)$$

where K is the apparatus function, I_L is the incident laser power, and α is the heat conversion efficiency, namely, the fraction of energy released as the heat against the energy absorbed. A is the absorbance of the sample at the excitation wavelength (248 nm), and the $1 - 10^{-A}$ term represents the absorptivity of the sample at 248 nm. The incident laser power dependence and the absorptivity dependence of the total (U_t) and the U_Δ (closed square) signal intensities of 6-AU were measured (Figure 10). The plots show good linear relations, so that the results could be analyzed with eq 5. The TRTL measurement for 2-HBP was also carried out under exactly the same experimental condition, shown as open circle in Figure 10b. From the ratio between the two slopes of the UI_L^{-1} values of 6-AU and 2-HBP in Figure 10b, the α value of 6-AU was determined to be 0.98 ± 0.01. Almost all the energy of 6-AU absorbed was found to be released as heat into solvent. The yield (Φ_Δ) for the photosensitization to form O_2 ($^1\Delta_g$) can be expressed as follows,

$$\Phi_\Delta = \frac{U_\Delta/\{I_L^{6-\mathrm{AU}}(1 - 10^{-A^{6-\mathrm{AU}}})\}}{U_{2-\mathrm{HBP}}/\{I_L^{2-\mathrm{HBP}}(1 - 10^{-A^{2-\mathrm{HBP}}})\}}(E_{ex}/E_\Delta) \quad (6)$$

Here $U_{2\text{-HBP}}$ is the TRTL signal intensity of 2-HBP, E_Δ is the energy of O_2 ($^1\Delta_g$) (94.6 kJ/mol),[41] and E_{ex} is the energy of the excitation light (248 nm, 482 kJ/mol). From the ratio between the two slopes in Figure 10b (0.123 ± 0.003) and eq 6, the Φ_Δ value was estimated to be 0.63 ± 0.03. The Φ_Δ value of 6-AU in aerated acetonitrile was obtained to be 0.34 with relative intensity of the O_2 ($^1\Delta_g$) emission (Figure 9). This value is three times larger than that of uracil (0.13)[42] despite of shorter lifetime of ^{3}6-AU*, resulting from a quite high value of Φ_{ISC}^{6-AU}.

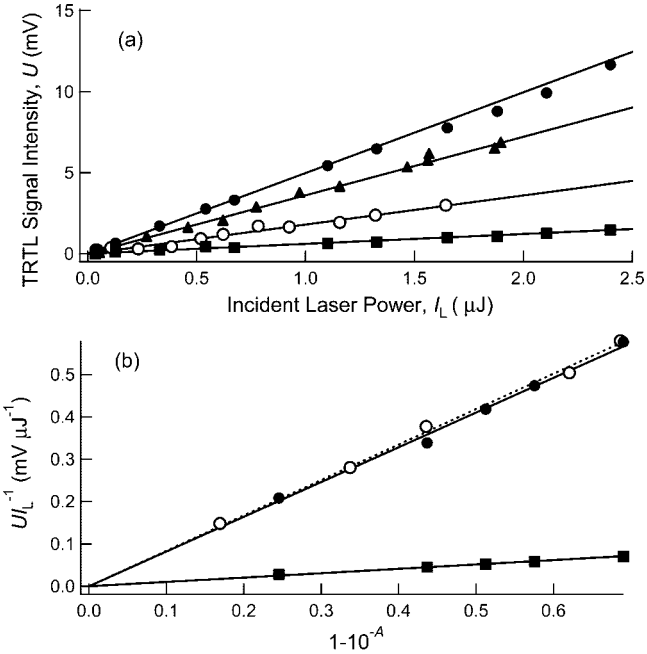

Figure 10. (a) Plots of the TRTL signal intensities for the U_t (closed circle: [6-AU] = 1.1×10^{-4} mol dm^{-3}, triangle: [6-AU] = 7.0×10^{-5} mol dm^{-3}, open circle: [6-AU] = 3.0×10^{-5} mol dm^{-3}) and U_Δ (square) of 6-AU ([6-AU] = 1.1×10^{-4} mol dm^{-3}) vs excitation laser power I_L. The solid lines were drawn by least-squares' fitting obtained with eq 5. (b) Plots of the UI_L^{-1} values for the U_t (closed circle), U_Δ (closed square) of 6-AU and U_t of 2-HBP (open circle). The dotted line shows the $\alpha = 1$ line determined by the result of the TRTL measurement of 2-HBP.

The Φ_Δ value also can be expressed with the kinetic rate constants of ^{3}6-AU*.

$$\Phi_\Delta = S_\Delta\Phi_{ISC}^{6-AU}k_q[O_2]/(k_0 + k_q[O_2]) \quad (7)$$

Here, S_Δ denotes the fraction of ^{3}6-AU* quenched by ground-state oxygen that results in the formation of O_2 ($^1\Delta_g$). The $k_q[O_2]/(k_0 + k_q[O_2])$ value can be estimated by the k_0 and the k_q values determined by the transient absorption measurement (Table 2) and the concentration of dissolved oxygen to be 0.81 in the O_2-saturated condition ([O_2] = 9.1×10^{-3} mol dm^{-3}).[29] Since 6-AU has a Φ_{ISC} value of unity, the S_Δ value can be roughly estimated to be 0.78. This large S_Δ value indicates that ^{3}6-AU* quenched by the dissolved molecular oxygen should be able to generate O_2 ($^1\Delta_g$) with high efficiency. This is the first report indicating that 6-AU would have a phototoxic property *in vivo*.

Excitation Wavelength Effect on the Quantum Yield for ISC. In the case of uracil, two mechanisms for the ISC process were proposed, from the $S_1(n\pi^*)$ state to the $T_1(\pi\pi^*)$ state and from the $S_2(\pi\pi^*)$ state to the $T_2(n\pi^*)$ state.[5,6,10] In order to estimate the quantum yield for Φ_{ISC} from the $S_1(n\pi^*)$ state, we carried out the transient absorption measurement using the 308 nm laser as an excitation light source. Since the energy of 308 nm (32500 cm^{-1}) is almost equal to the $S_1(n\pi^*)$ transition energy of 6-AU, predicted by our calculation (33000 cm^{-1}), the $S_1(n\pi^*)$ state 6-AU would be generated by the 308 nm excitation. The spectral feature and the decay rate constant (5.6×10^6 s^{-1}) of the transient were well agreed with those of ^{3}6-AU* obtained by the 248 nm excitation. Therefore, the transient obtained by the 308 nm excitation was safely assigned to the ^{3}6-AU*. To estimate the Φ_{ISC} value, the chemical actinometry with BP using the 308 nm laser as the excitation light source was also carried out in a similar manner described above. Then, the value of Φ_{ISC}^{6-AU} for the 308 nm excitation was successfully obtained to be 0.93 ± 0.04, which well agrees with the Φ_{ISC}^{6-AU} value estimated by the singlet oxygen formation yield (0.86 ± 0.04).

Additionally, on excitation at 308 nm, weak emission was observed, while there was no detectable emission on excitation at 248 nm. The emission peak was observed at 420 nm. The lifetime of the emission was shorter than our experimental time resolution (<30 ns); hence, the emission should be fluorescence from the excited singlet state of 6-AU, not phosphorescence from ^{3}6-AU*. Thus, the emission was likely to be from the $S_1(n\pi^*)$ surface of 6-AU. This aspect is supported by the fluorescence excitation spectrum (see Figure 1 inset). The quantum yield of the fluorescence (Φ_F) of 6-AU with 308 nm irradiation was estimated to be $(4.2 \pm 0.4) \times 10^{-3}$ in comparison with anthracene as a reference ($\Phi_F = 0.27 \pm 0.01$).[43] Similar experimental results on thymine and the uracil derivatives in the gas phase were reported by Kong et al.[11,12] They proposed that the excited uracil derivatives were trapped in a dark state, presumably $S_1(n\pi^*)$ state, and the fluorescence centered between 370 and 440 nm emitted and the lifetimes of this dark state were determined to be 22 ns for thymine.[11,12] Hare et al. also detected this $S_1(n\pi^*)$ state of another uracil derivative and the lifetime was at least several nanoseconds in aprotic solvents such as acetonitrile.[5]

Almost unity of the Φ_{ISC} value indicates that singlet → triplet ISC is predominant in the excited-state dynamics of 6-AU by the 308 nm irradiation. Addition to the ISC, internal conversion of $S_1(n\pi^*) \rightarrow S_0$ exists as a minor relaxation process (Φ_{IC} = 0.07).

Mechanism for Relaxation Process of 6-AU in the Excited State. Our experimental data clearly show that 6-AU has drastically different excited-state dynamics in comparison with uracil; the singlet → triplet ISC process is predominant for excited 6-AU while internal conversion to the S_0 state is the main relaxation pathway for excited uracil. Excitation of the $S_2(\pi\pi^*)$ state at the 248 nm results in dominant ISC to the triplet state with Φ_{ISC} of unity and produces no detectable fluorescence. On the other hand, direct excitation of the $S_1(n\pi^*)$ state at the 308 nm results in efficient ISC to the triplet state, $\Phi_{ISC} = 0.93$, and yields fluorescence with measured Φ_F of 4.2×10^{-3}. No detectable fluorescence with the 248 nm excitation suggests that ISC occurs directly from the $S_2(\pi\pi^*)$ state, or that IC from the $S_2(^1\pi\pi^*)$ state to the $S_1(^1n\pi^*)$ state is followed by rapid ISC from vibrationally hot $S_1(^1n\pi^*)$ state, prior to vibrational cooling. Hare et al. proposed the ultrafast IC mechanism from the vibrationally excited S_1 state in the study of the uracil derivatives.[5,6] Our experimental results obtained with the 308 nm irradiation clearly show that the ISC process is also dominant on the relaxation pathway of excited 6-AU from the Franck−Condon region of the $S_1(^1n\pi^*)$ state and it is in competition with the internal conversion process to the S_0 state.

In the case of uracil, two possible mechanisms for the internal conversion from initially excited $^1\pi\pi^*$ state were suggested; $^1\pi\pi^*/S_0$ and $^1\pi\pi^*/^1n\pi^*$.[3,7,8,13,14] And two possible mechanism for the ISC process were suggested; $^1n\pi^*/^3\pi\pi^*$ and $^1\pi\pi^*/^3n\pi^*$.[5,6,10] In the case of 6-AU, as is clear from our experimental results, the singlet → triplet ISC process is predominant and an involvement of the $^1\pi\pi^*/S_0$ internal conversion is remarkably low. For 6-AU, the energy difference between S_1 and T_1 is smaller than that between S_2 and T_2 (8900 and 9200 cm^{-1}, respectively). On the other hand, uracil has twice as large an energy difference between S_1 and T_1 as S_2 and T_2 (11000 and 5100 cm^{-1}, respectively). The energy difference between S_2 and T_2 of 6-AU is twice as large as that of uracil. This should lead to less involvement of $^1\pi\pi^*/^3n\pi^*$ ISC which was suggested in the quantum chemical calculation study of uracil.[10] Furthermore, based on our experimental results obtained with the 308 nm irradiation, it is clear that the $^1n\pi^*/^3\pi\pi^*$ ISC process is dominant on the relaxation of excited 6-AU.

To interpret the different Φ_{ISC} values between the 248 and 308 nm excitations, the following mechanism was proposed. Immediately after the 308 nm irradiation, 6-AU in the $S_1(^1n\pi^*)$ state, which would be vibronically excited, has the planar molecular structure as well as in the S_0 state and it would have had a significant spin−orbit coupling from early points along the nonradiative decay pathway of the $S_1(^1n\pi^*)$ state. Vibrationally hot $S_1(^1n\pi^*)$ state 6-AU populated by internal conversion from the $S_2(^1\pi\pi^*)$ state after the 248 nm irradiation also has significant spin−orbit coupling and more excess energy than that of the $^1n\pi^*$ state 6-AU directly excited by 308 nm light. Since vibrational cooling occurs more slowly when greater excess energy is present,[44,45] internal conversion from the $S_2(^1\pi\pi^*)$ state to the $S_1(^1n\pi^*)$ state is followed by rapid ISC from vibrationally hot $S_1(^1n\pi^*)$ state completely prior to vibrational cooling, in the case of the 248 nm excitation. This is the reason why no detectable fluorescence is produced with the 248 nm irradiation.

This idea that vibrationally hot $S_1(^1n\pi^*)$ state has a significant spin−orbit coupling is also in the study of the uracil derivatives by Hare et al. In the study, they also favored $^1n\pi^*/^3\pi\pi^*$ over $^1\pi\pi^*/^3n\pi^*$ ISC process and they postulated that ISC was in competition with vibrational cooling and spin−orbit coupling was significant only at early points along the nonradiative decay pathway of the $S_1(^1n\pi^*)$ state.[5,6] They also presumed that spin−orbit coupling in the relaxed $^1n\pi^*$ state might be smaller than that at early times due to the loss of planarity accompanying formation of the minimum energy $S_1(^1n\pi^*)$ state and the ISC did not occur from the vibrationally relaxed $S_1(^1n\pi^*)$ state.[5]

In the case of 6-AU excited by the 308 nm irradiation, we can not rule out a possibility of the ISC from the vibrationally relaxed $S_1(^1n\pi^*)$ state since its remarkably high Φ_{ISC} value. The ISC process might occur from the vibrationally relaxed $S_1(^1n\pi^*)$ state and be in competition with the internal conversion process to the S_0 state.

Two candidate mechanisms are proposed for the effect of the aza-substitution on the dynamics; acceleration of ISC process and inhibition of the ultrafast internal conversion. The first one is the acceleration of singlet → triplet ISC rate by introducing an N atom. As mentioned above, our calculation shows that the lone pair orbitals of the N6 and the O8 atoms contribute to HOMO-1 (see Figure 3). On the other hand, the π-type p_x atomic orbital on the N6 atom contributes to HOMO (the x axis is perpendicular to the molecular plane and the y axis corresponds to the direction of the N6 lone pair orbital). Thus, the $S_1(^1n\pi^*)$ → $T_1(^3\pi\pi^*)$ radiationless transition corresponding to a one-electron transition of the π electron (HOMO) into the n-orbital (HOMO-1) could occur near the N6 atomic nucleus. This one-center ISC is commonly known to aza-aromatics such as qunoxaline[46] and extensively studied by van der Waals et al.[47,48] This mechanism can explain the experimental results that the aza-substitution on uracil accelerates the ISC process. Additionally, the transition of the π electron into the n-orbital also could occur near the O8 atomic nucleus and this should be the main process of ISC in the case of uracil.

The second one is that the rigidity of the C5═N6 double bond should affect the internal conversion process to the S_0 state. For uracil the ultrafast internal conversion (<100 fs)[7,8] would take place through the conical intersection, and the nonplanar deformation equivalent to the twist around the double bound of C5═C6 was proposed to be important.[3,4,6−9] Gustavsson et al. reported that the calculated energetic cost for that out-of-plane rearrangement increased going from uracil through thymine to 5-fluorouracil in agreement with the ordering of the experimental $^1\pi\pi^*$ state lifetime. They suggested that a substitution stabilizing C5═C6 and C4═C5 π bonding prolonged the lifetime.[8] 6-AU has a C5═N6 double bond (1.293 Å) shorter than the C5═C6 double bond of uracil (1.354 Å). Vibrational spectrum measurement showed that 6-AU had higher frequencies of the ring out-of-plane vibrational mode (450 cm^{-1}) than uracil (435 cm^{-1}).[49] These results indicate that 6-AU should have a narrower and deeper potential curve along with the torsional axis of the C5═N6 double bond than uracil. Consequently, the rigidity of the *C*═N bond would prohibit the possibility going to the conical intersection, leading the effective ISC. The drastic increase of Φ_{ISC} by the 6-aza substitution strongly suggests that the twisting around the C5═C6 double bond is a key of the ultrafast internal conversion of uracil.

A further study will be necessary to fully understand the effect of the aza-substitution. However, for the first time, we clarified experimentally that a drastic change takes place to the excited-state dynamics of a nucleic acid base by the aza-substitution.

Conclusion

Excited-state dynamics of 6-AU in acetonitrile was studied with the transient absorption spectroscopy and the TRTL technique utilizing the 248 nm and the 308 nm laser excitation. It was found that 6-AU possesses very unique excited-state

dynamics different from uracil, a remarkably high yield for ISC with the 248 nm excitation (1.00 ± 0.10). The TRTL signal was also measured in acetonitrile, and quantum yield for the O_2 ($^1\Delta_g$) formation by the248 nm irradiation was estimated to be 0.63 ± 0.03.

Direct excitation of the "dark" S_1 ($n\pi^*$) state at 308 nm also results in efficient ISC to T_1 ($\pi\pi^*$) ($\Phi_{ISC} = 0.93 \pm 0.04$), and that 308 nm excitation yields fluorescence with measured Φ_F of 4×10^{-3}. These experimental results indicate that S_1 ($n\pi^*$) $\rightarrow T_1$ ($\pi\pi^*$) ISC process is dominant on the relaxation of excited 6-AU with UV irradiation. Two possible mechanisms for the considerably large Φ_{ISC} value due to the aza-substitution were proposed; acceleration of ISC process and inhibition of the ultrafast internal conversion. This is the first report to show clearly and experimentally that a drastic change takes place to relaxation mechanism of a nucleic acid base by the aza-substitution.

Although ultrafast measurements of the excited-state lifetime of nucleic acid bases and its derivatives have been done, variant interpretations of the experimental result have been reported and a comprehensive understanding of their relaxation processes is still under discussion. Here, we made the quantitative evaluation of the quantum yield for ISC and achieved a reliable knowledge about the relaxation processes of the excited 6-AU. To elucidate the excited-state dynamics, these quantitative evaluations of the quantum yield are also very important and an effective approach. To obtain a complete picture of the excited-state dynamics in 6-AU, ultrafast lifetime measurements of the excited singlet states would be significant, however, our work also can provide clear information on describing the picture.

Acknowledgment. The present work was partly financially supported in part by a Grant-in-Aid for Scientific Research (KAKENHI) on Priority Areas [477] "Molecular Science for Supra Functional Systems" from the Ministry of Education, Culture, Sports, Science and Technology (MEXT), Japan.

References and Notes

(1) Favre, A. In *Bioorganic Photochemistry: Photochemistry and the Nucleic Acids*; Morrison, H., Ed.; Wiley: New York, 1990.
(2) Crespo-Hernández, C. E.; Cohen, B.; Hare, P. M.; Kohler, B. *Chem. Rev.* **2004**, *104*, 1977.
(3) Matsika, M. *J. Phys. Chem. A* **2004**, *108*, 7584.
(4) Zgierski, M. Z.; Patchkovskii, S.; Fujiwara, T.; Lim, E. C. *J. Phys. Chem. A* **2005**, *109*, 9384.
(5) Hare, P. M.; Crespo-Hernández, C. M.; Kohler, B. *J. Phys. Chem. B* **2006**, *110*, 18641.
(6) Hare, P. M.; Crespo-Hernández, C. M.; Kohler, B. *Proc. Natl. Acad. Sci. U.S.A.* **2007**, *104*, 435.
(7) Gustavsson, T.; Sarkar, N.; Lazzarotto, E.; Markovitsi, D.; Improta, R. *Chem. Phys. Lett.* **2006**, *429*, 551.
(8) Gustavsson, T.; Bányász, Á.; Lazzarotto, E.; Markovitsi, D.; Scalmani, G.; Frisch, M. J.; Barone, V.; Improta, R. *J. Am. Chem. Soc.* **2006**, *128*, 607.
(9) Santro, F.; Barone, V.; Gustavsson, T.; Improta, R. *J. Am. Chem. Soc.* **2006**, *128*, 16312.
(10) Climent, T.; González-Luque, R.; Merchán, M.; Serrano-Andrés, L. *Chem. Phys. Lett.* **2007**, *441*, 327.
(11) He, Y.; Wu, C.; Kong, W. *J. Phys. Chem. A* **2003**, *107*, 5145.
(12) He, Y.; Wu, C.; Kong, W. *J. Phys. Chem. A* **2004**, *108*, 943.
(13) Merchán, M.; González-Luque, R.; Climent, T.; Serrano-Andrés, L.; Rodriguez, E.; Reguero, M.; Peláez, D. *J. Phys. Chem. B* **2006**, *110*, 26471.
(14) Hudock, H. R.; Levine, B. G.; Thompson, A. L.; Satzger, H.; Townsend, D.; Gador, N.; Ullrich, S.; Stolow, A.; Martínez, T. J. *J. Phys. Chem. A* **2007**, *111*, 8500.
(15) Clercq, E. D. *Antivir. Res.* **2005**, *67*, 56.
(16) Wagner, C. R.; Lyer, V. V.; Mclintee, E. J. *Cancer Res.* **1999**, *59*, 2944.
(17) Harada, Y.; Suzuki, T.; Ichimura, T.; Xu, Y.-Z. *J. Phys. Chem. B* **2007**, *111*, 5518.
(18) Skoda, J. *Prog. Nucl. Acid Res.* **1963**, *2*, 197.
(19) Roblin, R. O., Jr.; Lampen, J. O.; English, J. P.; Cole, Q. P.; Vaughan, J. R., Jr. *J. Am. Chem. Soc.* **1945**, *67*, 290.
(20) Schinder, R.; Welch, A. D. *Science* **1957**, *125*, 548.
(21) Schinder, B. I.; Frei, E.; Tuohy, J. H.; Gorman, J.; Freireich, E., Jr.; Clements, J. *Cancer Res.* **1960**, *20*, 28.
(22) Handschumacher, R. E.; Welch, A. D. *Cancer Res.* **1956**, *16*, 965.
(23) Kittler, L.; Löber, G. *Photochme. Photobiol.* **1969**, *10*, 35.
(24) Braslavsky, S. E.; Heibel, G. E. *Chem. Rev.* **1992**, *92*, 1381.
(25) Suzuki, T.; Kajii, Y.; Shibuya, K.; Obi, K. *Chem. Phys.* **1992**, *161*, 447.
(26) Suzuki, T.; Okuyama, U.; Ichimura, T. *J. Phys. Chem. A* **1997**, *101*, 7047.
(27) Omori, T.; Suzuki, T.; Ichimura, T. *Chem. Phys. Lett.* **1998**, *293*, 436.
(28) Suzuki, T.; Nagano, M.; Watanabe, S.; Ichimura, T. *J. Photochem. Photobiol. A* **2000**, *136*, 7.
(29) Murov, S. L.; Carmichael, I.; Hug, G. L. *Handbook of Photochemistry*, 2nd ed.; Marcel Dekker: New York, 1993.
(30) Miertus, S.; Scrocco, E.; Tomasi, *J. Chem. Phys.* **1981**, *55*, 117.
(31) Barone, V.; Cossi, M.; Tomasi, J. *J. Comput. Chem.* **1998**, *19*, 404.
(32) Frisch, M. J.; Trucks, G. W.; Schlegel, H. B.; Scuseria, G. E.; Robb, M. A.; Cheeseman, J. R. ; Montgomery, J. A., Jr.; Vreven, T.; Kudin, K. N.; Burant, J. C.; Millam, J. M.; Iyengar, S. S.; Tomasi, J.; Barone, V.; Mennucci, B.; Cossi, M.; Scalmani, G.; Rega, N.; Petersson, G. A.; Nakatsuji, H.; Hada, M.; Ehara, M.; Toyota, K.; Fukuda, R.; Hasegawa, J.; Ishida, M.; Nakajima, T.; Honda, Y.; Kitao, O.; Nakai, H.; Klene, M.; Li, X.; Knox, J. E.; Hratchian, H. P.; Cross, J. B.; Bakken, V.; Adamo, C.; Jaramillo, J.; Gomperts, R.; Stratmann, R. E.; Yazyev, O.; Austin, A. J.; Cammi, R.; Pomelli, C.; Ochterski, J. W.; Ayala, P. Y.; Morokuma, K.; Voth, G. A.; Salvador, P.; Dannenberg, J. J.; Zakrzewski, V. G.; Dapprich, S.; Daniels, A. D.; Strain, M. C.; Farkas, O.; Malick, D. K.; Rabuck, A. D.; Raghavachari, K.; Foresman, J. B.; Ortiz, J. V.; Cui, Q.; Baboul, A. G.; Clifford, S.; Cioslowski, J.; Stefanov, B. B.; Liu, G.; Liashenko, A.; Piskorz, P.; Komaromi, I.; Martin, R. L.; Fox, D. J.; Keith, T.; Al.Laham, M. A.; Peng, C. Y.; Nanayakkara, A.; Challacombe, M.; Gill, P. M. W.; Johnson, B.; Chen, W.; Wong, M. W.; Gonzalez, C.; Pople, J. A. Gaussian, Inc.: Wallingford, CT, 2004.
(33) Singh, P.; Hodgson, D. J. *Acta Crystallogr.* **1974**, *B30*, 1430.
(34) Salet, C.; Bensasson, R. *Photochem. Photobiol.* **1975**, *22*, 231.
(35) Whillans, W.; Johns, H. E. *J. Am. Chem. Soc.* **1971**, *93*, 1358.
(36) Porter, G.; Dogra, S. K.; Loutfy, R. O.; Sugamori, S. E.; Yip, R W. *J. Chem. Soc., Faraday Trans. 1* **1972**, *68*, 1462.
(37) Tatake, V. G.; Desai, T. S.; Sane, P. V. *Photochem. Photobiol.* **1976**, *24*, 463 The phosphorescence spectrum of 6-AU was obtained with γ-irradiation in the pellet form of dry polycrystalline powder at 77 K by Tatake et al., though we could not observe no phosphorescence in solution with the 248 nm irradiation.
(38) Bensasson, R. V.; Gramain, J.-C. *J. Chem. Soc., Faraday Trans. 1* **1980**, *76*, 1801.
(39) Schmidt, R.; Seikel, K.; Brauer, H. D. *J. Phys. Chem.* **1989**, *93*, 4507.
(40) Watanabe, S.; Suzuki, T.; Ichimura, T. *Chem. Phys. Lett.* **2003**, *374*, 41.
(41) Clark, W. D. K.; Steel, C. *J. Am. Chem. Soc.* **1971**, *93*, 6347.
(42) Bishop, S. M.; Malone, M.; Phillips, D.; Parker, A. W.; Symons, C. R. *J. Chem. Soc, Chem. Commun.* **1994**, 871.
(43) Eaton, D. F. *Pure Appl. Chem.* **1988**, *60*, 1107.
(44) Laermer, F.; Elsaesser, T.; Kaiser, W. *Chem. Phys. Lett.* **1989**, *156*, 381.
(45) Elsaesser, T.; Kaiser, W. *Annu. Rev. Phys. Chem.* **1991**, *42*, 83.
(46) Kasha, M. *Discuss. Faraday Soc.* **1950**, *9*, 14.
(47) van der Waals, J. H.; De Groot, M. S. *The triplet state.*; Zahlan, A.: London, 1967; p 101.
(48) Schadee, R. A.; Schmidt, J.; van der Waals, J. H. *Chem. Phys. Lett.* **1976**, *41*, 435.
(49) Rai, J. N. *Indian J. Phys.* **1983**, *57B*, 241.

JP803096J